

# The Influence of Mechanical Milling on the Structure and Magnetic Properties of Sm-Fe-N Powder Produced by the Reduction-Diffusion Process

Jung-Goo Lee<sup>1\*</sup>, Seok-Won Kang<sup>1</sup>, Ping-Zhan Si<sup>2</sup>, and Chul-Jin Choi<sup>1</sup>

<sup>1</sup>Functional Materials Division, Korea Institute of Materials Science, Changwon 642-831, Korea

<sup>2</sup>College of Materials Science & Engineering, China Jiliang University, Hangzhou 310018, People's Republic of China

(Received 26 January 2011, Received in final form 31 March 2011, Accepted 1 April 2011)

In the present study, we systematically investigated the effect of mechanical milling on the magnetic properties of Sm<sub>2</sub>Fe<sub>17</sub>N<sub>x</sub> powders produced by the reduction-diffusion process. The Sm-Fe powders obtained by the reduction-diffusion process were composed of an Sm<sub>2</sub>Fe<sub>17</sub> single phase. After nitrogenation, the coercivity and saturation magnetization of the powders were 0.48 kOe and 13.32 kG, respectively. The particle size largely decreased down to less than 2 μm in diameter after ball milling for 30 hours. However, there is no evidence that the Sm<sub>2</sub>Fe<sub>17</sub>N<sub>x</sub> was decomposed to Sm-N and α-Fe even after ball milling for 30 hours. The coercivity was significantly improved up to 8.82 kOe after milling for 60 hours. However, the magnetization decreased linearly with the ball milling time.

**Keywords :** reduction-diffusion, Sm-Fe-N, magnetic powder, ball milling

## 1. Introduction

Since Nd<sub>2</sub>Fe<sub>14</sub>B was first reported in 1983, none of the intermetallic compounds are known to possess intrinsic magnetic properties surpassing those of Nd<sub>2</sub>Fe<sub>14</sub>B, except for Sm<sub>2</sub>Fe<sub>17</sub>N<sub>x</sub>, whose Curie temperature, saturation magnetization, uniaxial magnetocrystalline anisotropy are 750 K, 1.56T (at 300 K), 12 MA m<sup>-1</sup> (at 300 K), respectively [1-3]. The especially high uniaxial anisotropy, which is essential for high coercivity, makes Sm<sub>2</sub>Fe<sub>17</sub>N<sub>x</sub> a promising permanent magnetic material in recent years although it was first introduced by Coey *et al.* in 1990 [1]. Due to its potential application for commercial usage, many processes have been employed to produce high-performance Sm<sub>2</sub>Fe<sub>17</sub>N<sub>x</sub> magnetic powder. These processes can be divided into three steps for convenience, that is: preparation of Sm<sub>2</sub>Fe<sub>17</sub> alloy, nitrogenation of the alloy, and milling the nitrogenized alloy. For the preparation of the parent Sm<sub>2</sub>Fe<sub>17</sub> alloy, different processes such as melt-cast (M/C) [4-6], mechanical alloying (MA) [7], and reduction-diffusion (R-D) [8-10] have been employed. Among these techniques, the R-D process has significant advantages over the others from a practical viewpoint. It uses samarium

oxide as a starting material, which is much cheaper than metallic samarium. The grinding process necessary in the M/C process can be skipped because powders could be directly obtained by the R-D process. In addition, it is a low temperature process compared to M/C process. Due to the benefit of the abovementioned cost-performance, the R-D process has attracted much attention in recent years. Quite recently, we succeeded in preparing an Sm<sub>2</sub>Fe<sub>17</sub>N<sub>x</sub> magnetic powder by the R-D process and subsequent nitrogenation treatment [11, 12]. On the other hand, it is now well known that the magnetic properties of Sm<sub>2</sub>Fe<sub>17</sub>N<sub>x</sub> powders depend on the size and the shape of the powders [13, 14]. However, most of the related works are concerned with Sm<sub>2</sub>Fe<sub>17</sub>N<sub>x</sub> powders produced by the M/C process [15, 16], and there have been few reports on the effect of mechanical milling of Sm<sub>2</sub>Fe<sub>17</sub>N<sub>x</sub> powders produced by the R-D process.

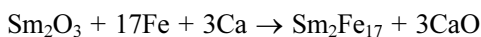
In the present study, we systematically investigated the effect of ball milling on the structure and magnetic properties of Sm<sub>2</sub>Fe<sub>17</sub>N<sub>x</sub> powders produced by the R-D process.

## 2. Experimental Procedure

Samarium oxide (Sm<sub>2</sub>O<sub>3</sub>) powder (Kojundo Chem., 99.99% purity) and iron (Fe) powder (Kojundo Chem., 99.9%

\*Corresponding author: Tel: +82-55-280-3606  
Fax: +82-55-280-3289, e-mail: jglee36@kims.re.kr

purity) were chosen as starting materials. First these were uniformly mixed with calcium (Ca) granules (Kojundo Chem., 99.5% purity) as a reductant using a 3-D mixer for 2 hours.  $\text{Sm}_2\text{O}_3$  and Ca were added in excess of stoichiometry to compensate for their loss due to their high vapor pressures during the R-D process. The content of  $\text{Sm}_2\text{O}_3$  and Ca in the mixed powders was 40% and 300% in excess of the chemical equivalent, respectively. The mixed powders were then pressed into 13 mm diameter pellets by applying a compaction pressure of 13 MPa with a quantity of 35 g per green body. Finally, the pellets are placed in a steel vessel, charged in a tubular furnace, and subjected to the R-D treatment at 1373 K for 6 hours under an argon atmosphere. During the R-D process,  $\text{Sm}_2\text{O}_3$  is reduced by Ca to Sm metal, which then diffuses into Fe powders to form Sm-Fe alloy powders. After the R-D treatment, the pellets consist of Sm-Fe mother alloy and CaO as described by the following equation;



The R-D treated pellets were moved into deionized water. Since CaO reacts with water to form hydroxide, the R-D treated pellets disintegrated into a water-alloy powder slurry. The Sm-Fe alloy powders were then obtained after calcium hydroxide was leached away with water. Fig. 1 shows a schematic diagram of the R-D process. Finally the alloy powders were washed with acetic acid and dried under vacuum conditions. The powders were then subjected to nitrogenization treatment. The temperature and time for nitrogenization was 723 K and 16 hours, respectively. The nitrogenization process was carried out in a 99.999%  $\text{N}_2$  atmosphere. After being nitrogenized, the powders were pulverized by balling milling in n-hexane. A stainless steel mill bottle of 1000  $\text{cm}^3$  and steel balls of  $\Phi$  5 mm were used with a ball to powder weight ratio of 20:1. The angular velocity was 250 rpm. The phases in the powders were determined by X-ray diffraction (XRD) using a  $\text{CuK}\alpha$  target at a scanning speed of  $2^\circ \text{min}^{-1}$ . The morphologies of the powders were examined by scanning electron microscopy (SEM). The magnetic properties were measured with a vibrating-sample magnetometer (VSM) at room temperature with a maximum applied field of 10

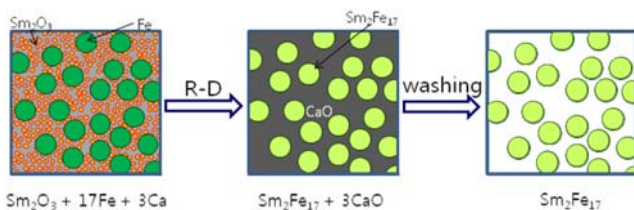


**Fig. 1.** Schematic illustration of the R-D process for the synthesis of  $\text{Sm}_2\text{Fe}_{17}$  powders.

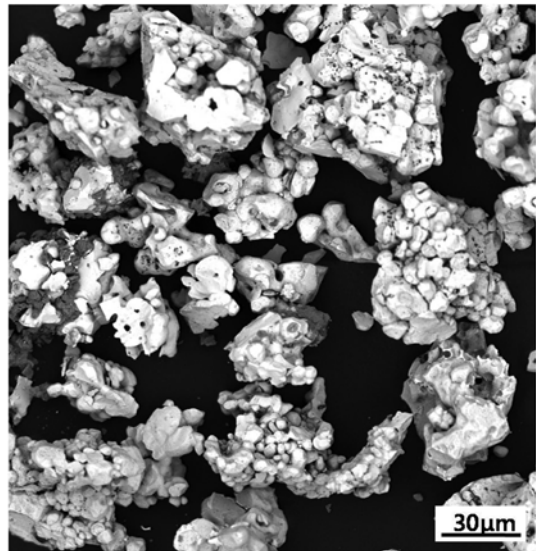


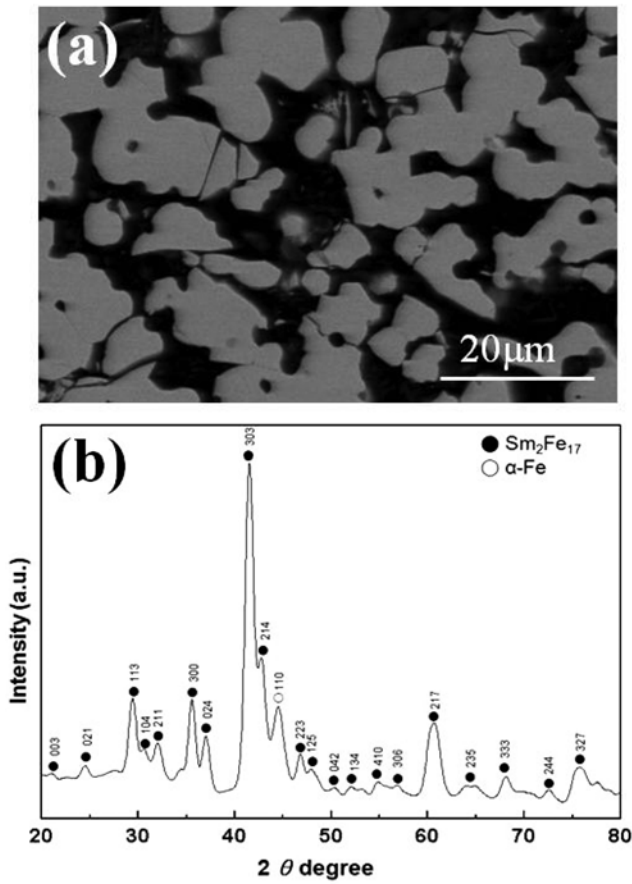
**Fig. 2.** Typical SEM image of Sm-Fe alloy powders produced by the reduction-diffusion process.

kOe. For VSM measurement, the powders were bonded with resin and magnetized in a magnetic field of 45 kOe.

### 3. Results and Discussion

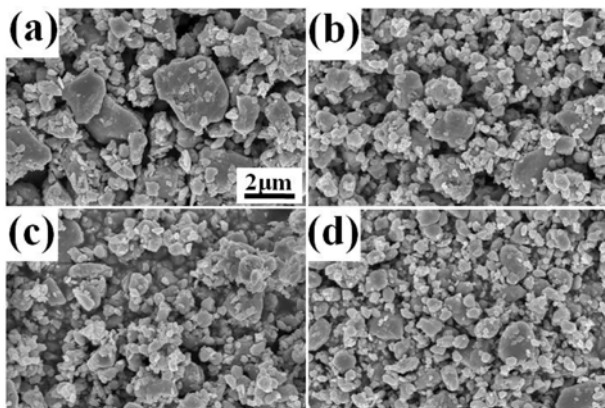
Fig. 2 shows a typical morphology of Sm-Fe alloy powders obtained by the R-D process. The powders consist of a lot of tiny particles corresponding to  $\text{Sm}_2\text{Fe}_{17}$  and pores. The pores in Sm-Fe alloy powders are considered to be formed after the removal of CaO from the R-D treated pellet by the washing process, which is consistent with the illustration in Fig. 1. The size of the  $\text{Sm}_2\text{Fe}_{17}$  particles is in the range of 5 to 10  $\mu\text{m}$ , which is a little bigger than that (3-5  $\mu\text{m}$ ) of Fe starting powders. The increase of the particle size could be attributed partly to Sm diffusion into the Fe powders and partly to sintering of the powders during the R-D process.

Fig. 3(a) and (b) show a typical cross-section SEM micrograph and XRD patterns of the R-D treated Sm-Fe alloy powders, respectively. It is noticed that no third phase such as  $\alpha$ -Fe,  $\text{SmFe}_3$  or  $\text{SmFe}_2$ , other than the  $\text{Sm}_2\text{Fe}_{17}$  phase is detected in the R-D treated Sm-Fe alloy powders. This is significantly different from that obtained by the melt casting process. The Sm-Fe alloy obtained by the latter process contains a lot of  $\alpha$ -Fe precipitates and Sm-rich phases, which needs heat treatment in a vacuum at a temperature of 950-1050  $^\circ\text{C}$  for a long time to remove them from the Sm-Fe alloy [13]. After nitrogenization, the coercivity of the  $\text{Sm}_2\text{Fe}_{17}\text{N}_x$  powders was 0.48 kOe. To improve the magnetic properties of the  $\text{Sm}_2\text{Fe}_{17}\text{N}_x$  powders, they were subjected to the ball milling process.



**Fig. 3.** Typical cross-section SEM image (a) and XRD patterns (b) of the R-D treated Sm-Fe alloy powders.

The change in particle size and shape of the  $\text{Sm}_2\text{Fe}_{17}\text{N}_x$  powders during the ball milling is shown in Fig. 4. The particles largely decreased in size after ball milling for 10 hours. However, they had a broad size distribution and irregular shape as shown in Fig. 4(a). By further ball milling, the size distribution and shape of the powders became narrower and more spherical with an increase in



**Fig. 4.** Typical SEM images of  $\text{Sm}_2\text{Fe}_{17}\text{N}_x$  powders after ball milling for 10, 30, 50, and 60 hours.

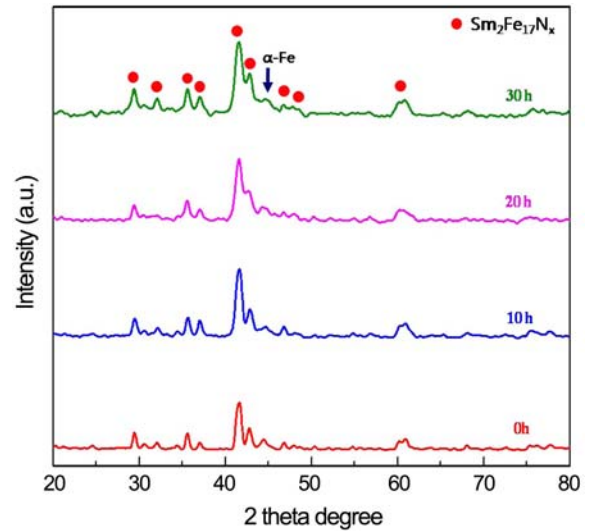


**Fig. 5.** XRD patterns of  $\text{Sm}_2\text{Fe}_{17}\text{N}_x$  powders before and after ball milling for 10, 20, and 30 hours.

milling time as shown Fig. 4. The particle size after ball milling for 30 hours was smaller than  $2\ \mu\text{m}$  in diameter.

It was reported that ball milling can result in the structural transformation of intermetallic powders [17]. Fig. 5 shows the XRD patterns of the powders before and after ball milling for 10, 20, and 30 hours. There was an amount of  $\alpha\text{-Fe}$  in as-nitrogenized  $\text{Sm}_2\text{Fe}_{17}\text{N}_x$  powders. This is attributed to oxidation of the powders during nitrogenation because the  $\text{Sm}_2\text{Fe}_{17}$  can be decomposed to Sm oxide and  $\alpha\text{-Fe}$  by oxidation. In addition, it seems that the intensity of the peak corresponding to  $\alpha\text{-Fe}$  slightly increased with ball milling time, which could be a result of oxidation of the powders during or after ball milling. However, there is no evidence that the  $\text{Sm}_2\text{Fe}_{17}\text{N}_x$  was decomposed into Sm-N and  $\alpha\text{-Fe}$  even after ball milling for 30 hours.

Figure 6 shows the dependence of the magnetic properties of  $\text{Sm}_2\text{Fe}_{17}\text{N}_x$  powders on the ball milling time.

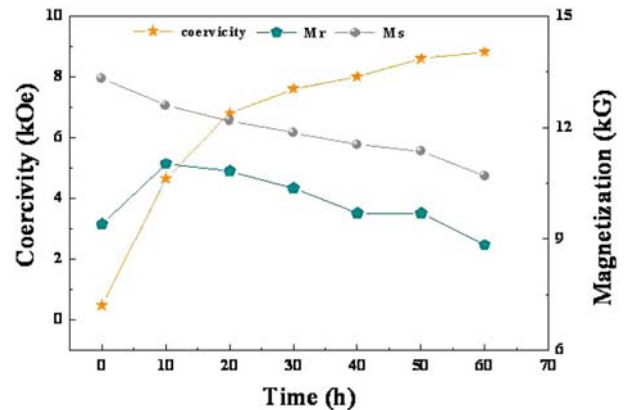


**Fig. 6.** Dependence of the magnetic properties of  $\text{Sm}_2\text{Fe}_{17}\text{N}_x$  powders on the ball milling time.

**Table 1.** Dependence of particle size, and magnetic properties of the  $\text{Sm}_2\text{Fe}_{17}\text{N}_x$  powder on ball milling time.

Milling time (h)	Average particle size ( $\mu\text{m}$ )	Magnetic Property		
		Ms (kG)	Mr (kG)	Hc (kOe)
0		13.32	9.4	0.48
10	1.23	12.60	11.02	4.65
30	0.84	11.86	10.37	7.60
50	0.75	11.36	9.69	8.60
60	0.61	10.70	8.84	8.82

The coercivity was significantly improved from 0.48 kOe before milling to 8.82 kOe after milling for 60 hours. The improvement of the coercivity of the  $\text{Sm}_2\text{Fe}_{17}\text{N}_x$  powder is attributed to the size reduction by ball milling. It should be noted here that the coercivity quickly increased in the early stages of ball milling, and then gradually increased with the ball milling time. This is because the ball milling efficiency is higher in the early stages compared to that in the later stages of the ball milling. The coercivity of  $\text{Sm}_2\text{Fe}_{17}\text{N}_x$ , it is reported to be inversely proportional to the particle size [18]. In addition, the single magnetic domain size,  $D_c$ , is known  $\sim 0.3 \mu\text{m}$  [19, 20]. Therefore, it is expected that a much higher coercivity can be achieved by further milling. On the other hand, the magnetization linearly decreased with ball milling time due to oxidation or lowering of the crystallinity induced by ball milling. The change in particle size and magnetic properties by the ball milling are summarized in Table 1.

#### 4. Conclusion

In the present study, the effect of ball milling on the structure and magnetic properties was systematically studied with  $\text{Sm}_2\text{Fe}_{17}\text{N}_x$  powders produced by the reduction-diffusion process.  $\text{Sm}_2\text{Fe}_{17}$  alloy powders were successfully produced by the reduction-diffusion process. After nitro-genization, the coercivity and saturation magnetization of the  $\text{Sm}_2\text{Fe}_{17}\text{N}_x$  powders was 0.48 kOe and 13.32 kG, respectively. The coercivity of the powders, however, was significantly improved up to 8.82 kOe after milling for 60 hours. There was no evidence that the  $\text{Sm}_2\text{Fe}_{17}\text{N}_x$  was decomposed to Sm-N and  $\alpha$ -Fe even after prolonged exposure to ball milling. Also, the magnetization linearly decreased with ball milling time.

#### Acknowledgments

This research was supported by a grant from the Fundamental R&D Program for Core Technology of Materials funded by the Ministry of Knowledge Economy, Republic of Korea and NSFC (10874159, 11074227).

#### References

- [1] J. M. Coey and H. Sun, *J. Magn. Mater.* **87**, L251 (1990).
- [2] Y. Otani, D. P. F. Hurley, H. Sun, and J. M. D. Coey, *J. Appl. Phys.* **69**, 5584 (1991).
- [3] J. Ye, F. Li, Y. Liu, S. Gao, and M. Tu, *J. Rare Earth* **23**, 53 (2005).
- [4] N. Imaoka, T. Iriyama, S. Itoh, A. Okamoto, and T. Katsumata, *J. Alloy. Compd.* **222**, 73 (1995).
- [5] H. Uchida, T. Yanagisawa, S. Kise, S. Tachibana, T. Kawanabe, Y. Matsumura, V. Koeninger, H. H. Uchida, Y. Miyamoto, H. Kaneko, and T. Kurino, *J. Alloy. Compd.* **222**, 33 (1995).
- [6] C. Cui, J. Sun, R. Wang, and Z. Liang, *Superlattices and Microstructures* **39**, 406 (2006).
- [7] K. Schnitzke, L. Schultz, J. Wecker, and M. Katter, *Appl. Phys. Lett.* **57**, 2853 (1990).
- [8] T. Y. Liu, W. C. Chang, C. J. Chen, T. Y. Chu, and C. D. Wu, *IEEE Trans. Magn.* **28**, 2593 (1992).
- [9] A. Kawamoto, J. Soyama, M. D. V. Felisberto, R. Hesse, A. V. A. Pinto, T. R. Taylor, and P. A. P. Wendhausen, *IEEE Trans. Magn.* **35**, 3322 (1999).
- [10] J. C. Boareto, T. Ishikawa, S. Yasuda, K. Takeya, K. Ishizaka, T. Iseki, and K. Ohmori, *Mater. Sci. For.* **534-536**, 1365 (2007).
- [11] H. Kwak, J. G. Lee, and C. J. Choi, *J. Kor. Powder Metall. Inst.* **16**, 336 (2009).
- [12] J. G. Lee, S. W. Kang, S. J. Park, Y. W. Oh, and C. J. Choi, *Kor. J. Met. Mater.* **48**, 842 (2010).
- [13] P. A. P. Wendhausen, B. Gebal, D. Eckert, and K. H. Muller, *J. Appl. Phys.* **75**, 6018 (1994).
- [14] K. Kobayashi, R. Skomski, and J. M. D. Coey, *J. Alloy. Compd.* **222**, 1 (1995).
- [15] K. Machida, A. Shiomi, H. Izumi, and G. Adachi, *Jpn. J. Appl. Phys.* **34**, L741 (1995).
- [16] K. Majima, M. Ito, S. Katsuyama, and H. Nagai, *J. Appl. Phys.* **81**, 4536 (1997).
- [17] S. Kwon, C. H. Kim, J. S. Kim, and J. C. Kim, *J. Cera. Soc. Japan* **114**, 934 (2006).
- [18] K. Kobayashi, T. Iriyama, T. Yamaguchi, H. Kato, and Y. Nakagawa, *J. Alloys Compd.* **193**, 235 (1993).
- [19] J. Hu, T. Dragon, M.-L. Sartorelli, and H. Kronmuller, *Phys. Status Solidi A* **136**, 207 (1993).
- [20] T. Mukai and T. Fujimoto, *J. Magn. Mater.* **103**, 165 (1992).